Single-Molecule Visualization of Environment-Sensitive Fluorophores Inserted into Cell Membranes by Staphylococcal γ-Hemolysin†

Anh Hoa Nguyen,‡,§,|| Vananh T. Nguyen,‡,|| Yoshiyuki Kamio,‡ and Hideo Higuchi*,§

Laboratory of Applied Microbiology, Department of Microbial Biotechnology, Graduate School of Agricultural Science, Tohoku University, Sendai 981-8555, Japan, and Biomedical Engineering Research Organization, Tohoku University, Sendai 980-8575, Japan

Received July 20, 2005; Revised Manuscript Received December 28, 2005

ABSTRACT: Single-molecule imaging of the entrance of a protein into the hydrophobic environment of a cell membrane was investigated. The pre-stem of LukF, one of the two components of the pore-forming toxin staphylococcal γ-hemolysin, was specifically labeled with 6-bromoacetyl-2-dimethylaminonaphthalene (Badan), an environment-sensitive fluorophore. Incubation of this derivative with erythrocyte ghost membranes resulted in a pronounced increase in fluorescence indicating insertion of Badan into the hydrophobic interior of the lipid bilayers. However, the increase in fluorescence was completely dependent on the interaction of Badan-labeled LukF with the γ-hemolysin second component. Individual spots of Badan fluorescence on erythrocyte membranes were visualized that were associated with single pores. Analyses of the intensities of these fluorescent spots and their photobleaching independently showed that a single pore contained 3−4 LukF molecules. Thus, environment-sensitive fluorophore signals can be used to study the insertion of specific protein domains into cell membranes at the single-molecule lever, and the use of this approach in the present study revealed that a single γ-hemolysin pore opening contains at least three LukF molecules.

Recently, single-molecule imaging of proteins has been studied intensively, and it is believed that a number of novel data regarding multistep interactions of enzymes with substrates, proteins with proteins, or movements of proteins on membranes can only be obtained by using this approach (*1*−*4*). Probes for single-molecule imaging have been limited to several visible light-excitable fluorophores. Environment-sensitive fluorophores (ESF)[1] that require excitation with UV light for their fluorescence are powerful tools for detecting environmental changes, but their use for the study of single-molecule imaging has not been investigated. The use of ESF for single-molecule imaging requires a high sensitivity detection system as well as a good model of proteins that undergo conformational changes in response to a change in their environment.

Staphylococcal γ-hemolysin is a bacterial pore-forming toxin that consists of two components, LukF (leukocidin fast fraction) and HS (γ-hemolysin second component). These components are secreted as water-soluble monomers that cooperatively form ring-shaped pores that can insert into human and animal erythrocyte membranes (*5*−*8*). A single pore may contain 3 or 4 molecules of LukF and 3 or 4 molecules of HS (*9*−*12*). On the basis of the water-soluble structure of the LukF monomer (*7*, *13*), as well as the structure of the related α-hemolysin homoheptameric pore (*14*), it was suggested that the pre-stem of LukF remains on the outside of the cell membrane when LukF binds to the membrane as a monomer and that it is subsequently inserted into the hydrophobic interior of the membrane to form functional pores as a result in a conformational change in LukF. The dramatic change in the environment surrounding the pre-stem of LukF appears to be controlled by the interaction of LukF with the HS component. Thus, the γ-hemolysin toxin is an ideal system for testing the application of ESF for the study of single-molecule imaging.

We recently determined that (*15*, *16*) oligomerization of γ-hemolysin involves various intermediate stages based on single fluorescence resonance energy transfer between pairs of acceptor and donor fluorophores attached to LukF and HS. However, these studies could not identify at which intermediate stage the insertion of γ-hemolysin components into human red blood cells (HRBC) membranes took place. To answer this question, a mutation in the structural gene for LukF was constructed that encoded a single cysteine in the pre-stem domain, and this residue was labeled specifically with the environment-sensitive fluorophore 6-bromoacetyl-2-dimethylaminonaphthalene (Badan). The binding of labeled LukF to HRBC membranes at the single-molecule level in the absence or presence of HS was then monitored by total internal reflection fluorescent microscopy (TIRFM). The

† The research was supported by Grants-in-Aid for Scientific Research (Y.K. and H.H.) and a scholarship (V.T.N.) from the Japan MEXT. The research was also supported by the Special Coordination Funds (H.H.) and a postdoctoral scholarship (H.A.N.) from the Japan Society for the Promotion of Science.

* Address correspondence to this author at the Biomedical Engineering Research Organization, Tohoku University, Aramaki-aza-aoba, Aoba-ku, Sendai, Miyagi 980-8578, Japan. Tel +81-22-795-4735; fax +81-22-795-5753; e-mail higuchi@material.tohoku.ac.jp.

‡ Laboratory of Applied Microbiology, Department of Microbial Biotechnology, Graduate School of Agricultural Science.

§ Biomedical Engineering Research Organization.

|| These authors contributed equally to this work.

[1] Abbreviations: au, arbitrary units; ESF, environment-sensitive fluorophores; LukF, leukocidin fast fraction; HS, γ-hemolysin second component; HRBC, human red blood cells; TIRFM, total internal reflection fluorescent microscopy.

10.1021/bi0514156 CCC: $33.50
Published on Web 02/04/2006

results of the experiments presented here are the first demonstration of protein entrance into the hydrophobic environment of a cell membrane at the single-molecule level with an environment-sensitive probe. In addition, these data provide a quantitative description of how the γ-hemolysin toxin pores insert into cell membranes, and they support the conclusion that this approach can be employed for gaining insights into mechanisms involved in other membrane-bound protein interactions.

MATERIALS AND METHODS

Preparation of Proteins. The T136C mutation was constructed on the basis of two considerations: (i) the crystal structure of the LukF stem domain in the water-soluble form and the crystal structure of the α-hemolysin in pore-formation form (*7*, *14*) (Figure 1A) and (ii) the fact that inhibition of the structural change in pre-stem of LukF by formation of a disulfide bond in the double-cysteine mutant T117C/T136C abolished pore formation on the cell membranes (*17*). The expression, purification, and labeling of the cysteine mutant, $LukF_{136C}$, with Badan were performed as previously described (*15*). The labeling efficiency was ~96% as determined by the absorbance of the derivative at 390 nm. The presence of free fluorophore was negligible as no band of free fluorophore was detected by SDS−PAGE (Figure 1B, lane 3, UV illumination). A cysteine residue was also introduced into LukF at S45 ($LukF_{45C}$) located at the top of the cap domain of LukF, and this construct was also labeled with Badan to yield $LukF_{45C}Bd$ (Figure 1A,B). The $LukF_{45C}$-Bd derivative served as a negative control since, unlike the pre-stem region of LukF, it was expected that the top of the cap domain would remain outside the membranes following formation of pores.

Hemolytic Titration Assay. Hemolytic assays of LukF mutant proteins together with HS were performed using HRBC (1% cells/volume) in phosphate-containing saline buffer at pH 7.4 as described previously for the wild-type proteins (*17*, *18*).

Assay for Determining Shifts in the Emission Profile of Badan. Badan-labeled LukF (30 nM) was incubated with or without erythrocyte ghost cell membranes, either in the presence or in the absence of HS, for 30 min in phosphate-containing saline buffer. The fluorescence of Badan-labeled proteins was detected using a spectrofluorometer (Jasco). Spectra were obtained using an excitation wavelength of 408 nm and by measuring the emission at wavelengths from 435 to 600 nm. All spectra were corrected for background emission using the appropriate buffer blanks.

Single-Molecule Imaging of Membrane Insertion. Sample preparation, settings of TIRFM, imaging, and data analysis were performed as described previously (*15*, *16*). In brief, various concentrations of $LukF_{136C}Bd$ were mixed with HS to give a final molar ratio of 1:9, and the mixtures were incubated with 1% HRBC in phosphate-containing saline buffer at 25 °C for 30 min. Samples containing toxin-bound ghost erythrocytes were excited by a NEO ARK blue laser at 408 nm, and the resulting fluorescence of longer 435 nm was observed under TIRFM (*15*) using plan Apo × 60 N. A. 1.4 objective (Olympus), a 435 nm long pass filter and SIT camera (Hamamatsu Photonics, C2400−08) with an image intensifier (VS4-1845, Video Scope). Signal analyses were conducted using Macro software and Scion free software.

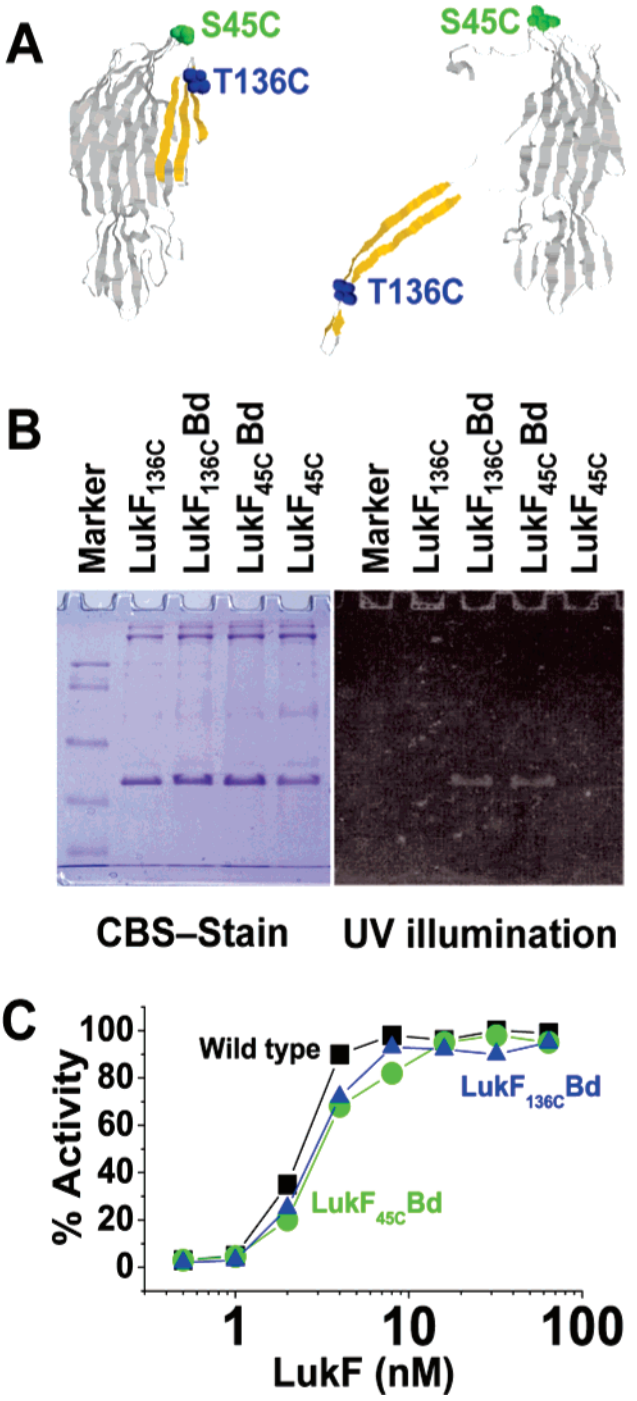

FIGURE 1: Structures and labeling of genetically altered LukF. (A) Position of T136 (blue) and S45 (green) on the crystal structure of LukF in the water-soluble conformation (left) and the pore-formation conformation (right) (*7*, *14*). (B) SDS−PAGE gels of Badan-labeled and unlabeled $LukF_{T136C}$, stained with Coomassie brilliant blue (left), or visualized under UV light (right). Each lane was loaded with 10 μg of protein. (C) Hemolytic activity of wild-type LukF and labeled LukF mutants.

The glass chamber for sample preparation was assembled using a quartz glass slide, a cover slip and two spacers (25 μm thick). These items were sonicated with 0.1 M KOH and 5 M HCl, and then rinsed with distilled water before use to reduce the background autofluorescence (*19*). A pinch hole was made to illuminate only 30 μm^2 of the sample

during focusing in order to avoid the unnecessary photobleaching of Badan.

RESULTS

Preparation of Badan-Labeled LukF Mutants. To monitor the insertion of LukF into lipid bilayers during the formation of pores, the pre-stem of LukF was specifically labeled with Badan, an environment-sensitive fluorophore, since the insertion process was expected to be accompanied by a conformational change in this domain (*7*, *17*, *20*, *21*). Thus, it was anticipated that the insertion of Badan would be reflected by a shifting of its emission spectra and/or by an increase in the intensity of its emission (*22*). Since LukF does not contain any cysteine residues, the labeling of LukF with Badan was made possible by introduction of a cysteine into LukF at T136 near the turns of the pre-stem domain ($LukF_{136C}$), a position expected to be within the hydrophobic interior of the lipid bilayer when the stem domain inserts into membranes to form pores (Figure 1A). The mutant $LukF_{136C}$ protein was specifically labeled at the introduced cysteine with Badan to generate $LukF_{136C}Bd$, and the derivative protein was then purified to remove free Badan (Figure 1B). A cysteine residue was also introduced into LukF at S45 ($LukF_{45C}$) located at the top of the cap domain of LukF, and this construct was also labeled with Badan to yield $LukF_{45C}Bd$ (Figure 1A,B). The $LukF_{45C}Bd$ derivative served as a negative control since, unlike the pre-stem region of LukF, it was expected that the top of the cap domain would remain outside the membrane following formation of pores.

The mole ratio of Badan/LukF in the Badan-labeled LukF preparations was 0.96:1, thus indicating a high labeling efficiency. The hemolytic activities of these preparations were similar to that of wild-type protein (~3 nM LukF caused 50% hemolysis against 6×10^{10} HRBC/L), suggesting that both Badan and the introduced cysteine had no significant effect on the formation of functional pores (Figure 1C).

Hydrophobic Sensitivity of Labeled Badan. The "water-soluble" structure of LukF shares some basic structural features with the membrane-inserted subunit (protomer) of the related staphylococcal α-hemolysin, except that the stem domain of "water-soluble" LukF folds back to the core structure (*7*) while the stem domain of "membrane-inserted" α-hemolysin protomer (*14*) projects from the core structure and is inserted into lipid bilayers. On the basis of the amino acid sequence homology of the these proteins (*23*) and similarities in the core structures of LukF and α-hemolysin (*7*), Thr136 of LukF was shown to correspond to Val140 of α-hemolysin stem domain. Since the predicted 3D structure of α-hemolysin in lipid membranes indicates that Val140 is located within the lipid bilayer (*14*), it follows that Thr136 of LukF would also be expected to insert into the membrane of HRBC whenever γ-hemolysin pores are formed.

In the absence of HS, LukF binds as a monomer to the HRBC membrane without the membrane insertion of the pre-stem domain (*7*, *17*). Accordingly, the spectrum and intensity of emission by $LukF_{136C}Bd$ were measured at the monomeric stage of pore formation on HRBC membranes in order to determine whether the Badan on $LukF_{136C}Bd$ could be used as a signal to monitor the insertion of pre-stem domain into

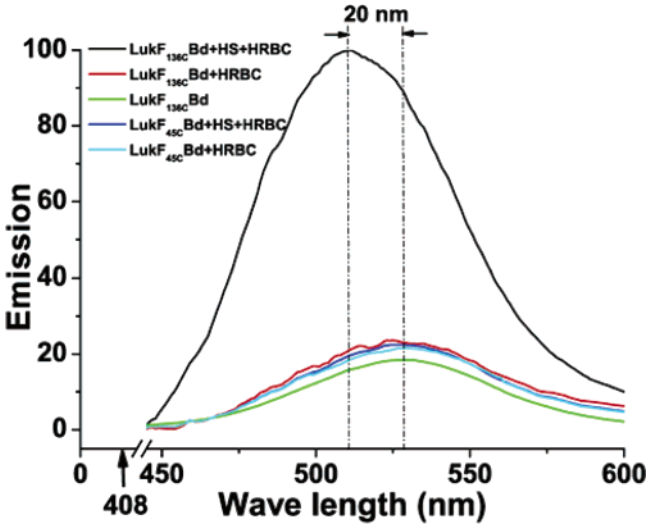

FIGURE 2: Effect of environment on the fluorescence emission spectra and intensity of Badan-labeled LukF. The relative emission spectra of Badan-labeled LukF bound to HRBC was measured in the presence or absence of HS.

lipid bilayers (*20*, *21*). These experiments revealed that there was no shift in the emission maximum and only a minor increase in the emission intensity (~1.3-fold) upon binding of the monomer to HBRC membranes as compared to incubation of $LukF_{136C}Bd$ in aqueous buffer in the absence of HRBC (Figure 2). In contrast, the addition of HS to the incubation mixtures containing both $LukF_{136C}Bd$ and HRBC membranes resulted in a dramatic increase in the emission intensity (5-fold) of $LukF_{136C}Bd$, and this was accompanied by a blue shift in the emission spectra of approximately 20 nm (Figure 2). These spectral changes are similar to those observed when $LukF_{136C}Bd$ was incubated with methanol (data not shown). Neither an increase in emission intensity nor a shift in the emission peak was detected when similar experiments were conducted with $LukF_{45C}Bd$ (Figure 2).

The method, used to verify that Acrylodan (a dimethylaminonaphthalene derivative, similar to Badan) actually interacts with lipid bilayers described by Valeva and colleagues (*20*), was employed to verify for Badan in our experiment. Briefly, deoxycholate (DOC) was used to solubilize erythrocyte membranes that had been previously incubated with $LukF_{136C}Bd$ and HS, and the intensity of Badan fluorescence was determined by fluorospectrometry before and after addition of DOC. An increase in emission intensity and a shift in the emission spectra of $LukF_{136C}Bd$ was detected in the presence of HRBC and HS. However, these changes were reversed following delipidation with DOC, thus indicating that Badan linked to the stem domain had indeed inserted into the hydrophobic lipid bilayer of the HRBC membrane. Furthermore, examination of the delipidated sample by TIRFM revealed that the $LukF_{136C}Bd$ in the sample could not be observed as discrete regions of fluorescence. These observations support the conclusion that the change in the fluorescence of Badan is due to the insertion of residue 136 of $LukF_{136C}Bd$ into the membrane. These data further indicate that $LukF_{136C}Bd$ can be used as a reporter to monitor the insertion of pre-stem domain of LukF into the hydrophobic lipid bilayer of the HRBC membrane.

Single-Molecule Imaging of Badan. A highly sensitive camera was used to observe single-molecule signals of Badan

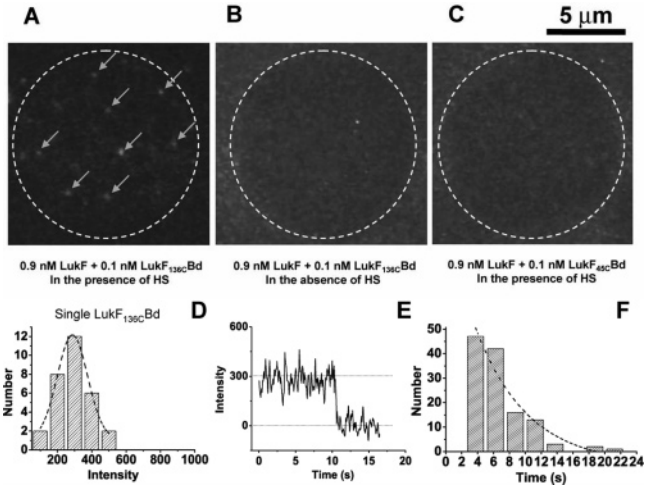

FIGURE 3: Single-molecule imaging of $LukF_{136C}Bd$. (A−C) Representative microphotos taken under TIRFM of ghost HRBC (bordered within dashed line circles) incubated with mixtures containing 0.1 nM $LukF_{136C}Bd$ and 0.9 nM unlabeled LukF. Note that fluorescent spots (arrows) were observed with $LukF_{136C}Bd$ in the presence of HS (A) but not with $LukF_{136C}Bd$ in the absence of HS (B) or with $LukF_{45C}Bd$ in the presence of HS (C). (D−F) Analyses of the fluorescent regions observed in panel A. (D) Intensity histogram fitted to a Gaussian curve (dashed line). (E) Intensity bleaching steps. (F) Histogram of bleaching times fitted to an exponential curve (an average time of 6.7 s was observed).

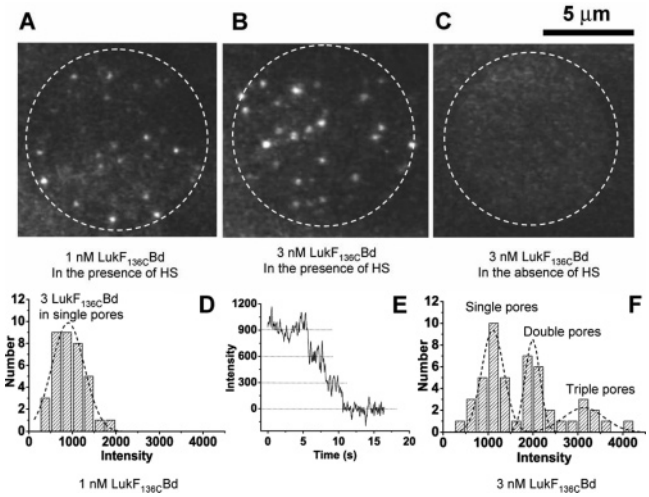

FIGURE 4: (A−C) Single pore formation by insertion of three or four $LukF_{136C}Bd$ molecules. Representative microphotos were taken under TIRFM of ghost HRBC (bordered within dashed line circles) incubated with 1 nM (A) or 3 nM (B) $LukF_{136C}Bd$ in the presence of HS or 3 nM $LukF_{136C}Bd$ in the absence of HS (C). (D) Intensity histogram of $LukF_{136C}Bd$ fluorescent regions obtained from the experiment shown in panel A. Data were fitted to a Gaussian curve (dashed line). (E) Three steps of the intensity bleaching of Badan in the experiment shown in (A). (F) Intensity histogram of $LukF_{136C}Bd$ spots taken from the experiment shown in panel B, the data being Gaussian fitted (dashed line).

upon insertion of the pre-stem domain of $LukF_{136C}Bd$ into the hydrophobic environment of the lipid bilayers as described previously (*15*). Preliminary experiments revealed that pretreatment of glass slides with 5 M HCl was a critical step for the reduction of background of autofluorescence. In addition, the blue light was let through a pinch hole to illuminate only 30 μm^2 of the sample during focusing in order to avoid the unnecessary photobleaching of Badan. Data were also obtained from an illuminated area of 1000 μm^2 near the focus area following removal of the pinch hole.

Recent studies suggest that LukF and HS assemble in HRBC membranes as pores, each of which contains 3 or 4 units of LukF and 3 or 4 units of HS (*9*−*12*). To observe $LukF_{136C}Bd$ as a single molecule in the HRBC membrane, the number of $LukF_{136C}Bd$ molecules able to contribute to the formation of single pores was minimized by diluting $LukF_{136C}Bd$ with unlabeled LukF to give a molar ratio of 1:9. A low concentration (1 nM) of the LukF−$LukF_{136C}Bd$ mixture was then incubated with HRBC in the presence of HS to form individual pores, and these were observed as distinct regions of fluorescence by TIRFM (Figure 3A). A single peak with a maximum at approximately 280 au (arbitrary units) was observed when the intensities of $LukF_{136C}Bd$ fluorescent spots were fitted to a Gaussian curve (Figure 3D). Most of these spots were bleached as a single step (90%, $n = 20$) (Figure 3E), suggesting that the fluorescence in these spots originated from single molecules of $LukF_{136C}Bd$. The histogram of the emission times of single $LukF_{136C}Bd$ molecules was fitted to an exponential curve (Figure 3F), giving an average emission time of about 6.7 s. These spots of fluorescence were not observed when similar experiments were carried out in the absence of HS (Figure 3B) or when $LukF_{45C}Bd$ was used (Figure 3C), thus confirming that the observed fluorescence in these spots was emitted by $LukF_{136C}Bd$ present in membrane-inserted pores. Taken together, we conclude that $LukF_{136C}Bd$ can be used as a model protein to monitor single molecules of a protein or polypeptide inserted into the hydrophobic environment of a lipid bilayer from a hydrophilic environment.

Observation of Single Membrane-Inserted Pore. We previously reported that LukF and HS oligomerize into intermediate LukF−HS heterodimers, then heterotetramers ($[LukF-HS]_2$), before forming a pore, which may be a heterohexamer ($[LukF-HS]_3$), a heteroheptamer (3LukF−4HS or 4LukF−3HS), or heterooctamer ($[LukF-HS]_4$), on the membranes of HRBC (*15*). However, it was unclear at what stage of oligomerization the insertion of the pre-stem domain of LukF into the lipid bilayers occurs. Thus, experiments were conducted in order to obtain this information. $LukF_{136C}Bd$ (1 nM) was incubated with HRBC in the presence of HS, and approximately 15 individual fluorescence regions per cell were observed (Figure 4A). A single peak at approximately 1000 au was observed when the intensities of these regions were fitted to a Gaussian curve (Figure 4D). This intensity was about 3.5 times higher than that observed for pores containing single $LukF_{136C}Bd$ molecules (280 au, Figure 3D). Therefore, in accordance with recent data (*9*−*12*), it is likely that each fluorescence region was associated with a single pore that contained approximately 3−4 molecules of $LukF_{136C}Bd$. This conclusion was supported by the examination of 60 fluorescent regions in order to determine the number of steps that resulted in the bleaching of their emission intensity. Thus, only three regions (5%) were bleached in two steps and nine regions (15%) were bleached in more than three steps, whereas 48 regions (80%) were bleached in three steps (Figure 4E). When the $LukF_{136C}Bd$ concentration was increased 3-fold to a concentration of 3 nM, on average approximately 24 distinct regions of fluorescence were observed per cell (Figure 4B), and this was accompanied by hemolysis. The fluorescent intensities these regions were distributed into several peaks that were multiples of approximately 1000 au

(Figure 4F), suggesting that fluorescent regions with intensities of approximately 2000 and 3000 au might represent the association of two and three pores, respectively. Indeed, a determination of the number of steps involved in the bleaching of the emission intensities of fluorescent regions with a peak at approximately 1000 au was in agreement with this conclusion. Thus, within 60 regions examined, four of these regions (approximately 7%) were bleached in two steps, 43 regions (72%) were bleached in three steps, and 13 regions (approximately 22%) were bleached in more than three steps. In contrast, a similar analysis of 20 fluorescent regions with peaks of approximately 2000 au or higher revealed that 95% of these regions were bleached in more than three steps. In addition, the fluorescence in the regions visualized in our experiments was specifically emitted as a result of the translocation of Badan into HRBC membranes, as indicated by the lack of fluorescence in the experiments where $LukF_{136C}Bd$ was incubated with HRBC in the absence of HS (Figure 4C) or, alternatively, when $LukF_{45C}Bd$ was incubated with HRBC in the presence of HS (data not shown).

DISCUSSION

Single-Molecule Observation of an ESF. Although the dependence of the intensity of fluorescence and the spectra of emission of ESF on a hydrophobic environment suggests they can potentially be powerful tools for investigating the formation of transmembrane pores/channels and other phase-dependent protein interactions—for example, membrane transport or the ligation of molecules to membrane-bound receptors—the application of ESF has thus far been limited by mass level detection (*20*−*22*). The use of ESF has been extended in this study into the single-molecular imaging methodology for visualization of protein functional insertion into a native cell membrane. An increase in the emission intensity and a shift in the emission spectra of $LukF_{136C}Bd$ were detected when this protein was incubated with HRBC membranes, and these changes were observed only when experiments were conducted in the presence of HS. These observations are in agreement with the HS-dependent insertion of the pre-stem domain of LukF into the hydrophobic lipid bilayers of HRBC membranes. In addition, distinct fluorescent regions were observed when mixtures of LukF (0.9 nM) and $LukF_{136C}Bd$ (0.1 nM) were incubated with HRBC and HS, and the intensity of emission of the majority of these regions was bleached in one step, thus indicating that these regions contained a single molecule of $LukF_{136C}Bd$. The observation that approximately 10% of these regions bleached in two steps is reasonable if we consider the Poisson distribution of $LukF_{136C}Bd$ into pores where each pore contained 3 or 4 molecules of LukF.

Insertion of LukF To Form a Pore. When $LukF_{136C}Bd$ at a concentration of 1 nM was incubated with HRBC in the presence of HS, the range of the intensities of fluorescence in fluorescent regions was distributed into a single peak. The peak had intensity at ~1000 au that was about 3.5 times greater than regions containing a single molecule of $LukF_{136C}Bd$. Most of these regions bleached in three or more steps, indicating that they contained 3 or 4 molecules of $LukF_{136C}Bd$. Considering the previous finding that one γ-hemolysin pore contains 3−4 molecules of LukF (*6*), these data strongly suggested that the observed fluorescent regions were single pores. About 5% of the regions were found to contain only 2 molecules of $LukF_{136C}Bd$; however, this is reasonable if we consider that a Poisson distribution predicts that the preparation of $LukF_{136C}Bd$ contained 4% unlabeled LukF. When similar experiments were conducted with $LukF_{136C}Bd$ at a final concentration of 3 nM, the range of the intensities of fluorescence in fluorescent regions was distributed into three peaks. The maximum fluorescence intensity of the first peak was approximately 1000 au, which suggests that it was derived from single pores. The maximum fluorescence intensities of other peaks were at even multiples of 1000 au, indicating they comprised groups of pores.

The formation of a γ-hemolysin pore in HRBC membranes involves two processes, the oligomerization of LukF and HS and the insertion of the oligomers into the membrane. We recently demonstrated that the oligomerization process includes formation of a LukF−HS heterodimer and a $[LukF-HS]_2$ heterotetramer (*15*). The mechanism of the membrane insertion process of γ-hemolysin is still unclear with regard to (i) the intermediate stage at which the insertion is initiated and (ii) how many stem domains contribute to the formation of a pore upon its insertion into the membrane.

Details regarding the mechanism involved in the initiation of insertion are lacking not only for γ-hemolysin, but also for other pore-forming toxins. Alternative models for membrane insertion have been proposed for pore-forming toxins (*24*). A prepore model, whereby monomers first oligomerize into a prepore that is subsequently inserted into the membrane via a specific transmembrane domain, has been proposed for *Clostridium septicum* α-hemolysin (*25*), *Clostridium perfringens* cytolysin (*26*, *27*), anthrax protective antigen (*28*), perfringolysin O (*29*, *30*), and aerolysin (*31*). By contrast, the "continuous growth model" was originally proposed for the pore-forming streptolysin O (*32*). According to this model, transmembrane domains of monomers are first inserted into the membranes, and the completed pore is then assembled in situ from membrane-localized monomers. Staphylococcal α-toxin and γ-hemolysin have been proposed to belong to the prepore model group, mostly on the basis of the observations that their mutants, in which transmembrane/stem domains were either truncated (*21*, *33*) or locked back to the core structure by disulfide bonds, could form artificial prepores (*17*, *34*). However, these observations do not eliminate the continuous model from consideration since the insertion of the stem domain had already been inhibited before the first stage of membrane-bound monomers. In the present study, direct observation of a single Badan label on the LukF pre-stem domain allowed us to distinguish between the intermediate oligomers, and we found that insertion does not occur at the heterodimer or heterotetramer stages.

There have been data suggesting a hexameric (*10*), heptameric (*9*), or octameric structure of γ-hemolysin pores, at least in the SDS-stable form (*11*, *12*). However, the question regarding how many stem domains insert into the cell membrane to form a functional pore has not previously been answered. The novel approach of ESF single-molecule imaging in this study brought us to the conclusion that a pore may contain 3 or 4 membrane-inserted LukF units, which in turn indicates the oligomer size of functional γ-hemolysin pores could be variable from hexamer to octamer. It is noteworthy that, in a difference from previous studies, the measurements in our study were carried out

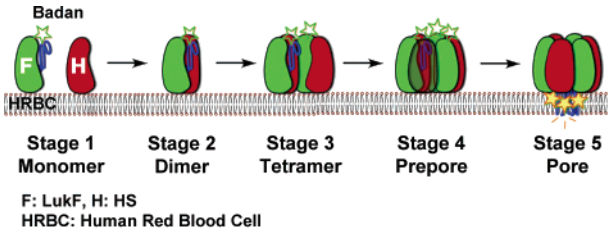

FIGURE 5: Model for the oligomerization of staphylococcal γ-hemolysin. In a solution containing LukF, HS, and HRBC, LukF binds on HRBC membranes with its stem domain folded back to the cap domain (stage 1). LukF then dimerizes with a HS to form a LukF−HS heterodimer without insertion of the stem domain into the bilayers of the HRBC membrane (stage 2). Two LukF−HS heterodimers are then oligomerrized to form a heterotetramer (stage 3). Succeeding oligomerization steps (stages 4) result in the association of additional heterodimers and monomers to form either hexameric $[LukF-HS]_3$, heptameric [3LukF−4HS or 4LukF−3HS], or octameric $[LukF-HS]_4$ oligomers to yield a prepore complex. Formation of the prepore complex is followed by a conformational change in the prepore proteins that result in the concerted insertion of three (or four) LukF stem domains into the HRBC membrane bilayers (stage 5).

directly on native cell membranes and in the physiological range of protein concentrations. On the basis of the results presented both here and in previous studies (*15*, *17*), we propose the following model for the formation of the γ-hemolysin functional pore (Figure 5). In a solution containing LukF, HS, and HRBC, LukF binds on HRBC with its stem domain folded back to the cap domain (stage 1). LukF then dimerizes with a HS to form LukF−HS heterodimer (stage 2). Two LukF−HS heterodimers are then oligomerized to form a heterotetramer (stage 3). Successive association of additional heterodimers and monomers giving rise to a complete ring-shaped oligomer, which may be a heterohexamer $[LukF-HS]_3$ or heteroheptamer [3LukF−4HS or 4LukF−3HS] or heterooctamer $[LukF-HS]_4$ (stage 4). Stages 2−4 occur without insertion of the stem domain into the HRBC membranes. However, when oligomerization is complete, a conformational change in the protein complex occurs that results in the concerted insertion of three or four LukF stem domains into the membrane (stage 5) to form a functional hydrophilic transmembrane pore/channel through the HRBC that allows the influx of water and hemolysis.

In conclusion, we demonstrate here for the first time the single-molecule imaging of a protein labeled with ESF, a novel class of fluorescence probes. It is anticipated that the information we obtained using this novel approach to determine how γ-hemolysin inserts its pores into the native cell membranes will be extremely useful for investigations of other membrane-bound protein interactions.

ACKNOWLEDGMENT

We thank Drs. H. B. Tran and Paul D. Rick for critical reading of the manuscript and T. M. Watanabe for providing us with software to analyze images of fluorescent signals.

REFERENCES

1. Funatsu, T., Harada, Y., Tokunaga, M., Saito, K., and Yanagida, T. (1995) Imaging of single fluorescent molecules and individual ATP turnovers by single myosin molecules in aqueous solution, *Nature 374*, 555−559.
2. Schütz, G. T., Kada, G., Pastushenko, V. P., and Schindler, H. (2000) Properties of Lipid Microdomains in a Muscle Cell Membrane Visualized by Single Molecule Microscopy, *EMBO J. 19*, 892−901.
3. Sako, Y., Minoghchi, S., and Yanagida, T. (2000) Single-molecule imaging of EGFR signaling on the surface of living cells, *Nat. Cell Biol. 2*, 168−172.
4. Haustein, E., and Schwille, P. (2004) Single-molecule spectroscopic methods, *Curr. Opin. Struct. Biol. 14*, 531−540.
5. Tomita, T., and Kamio, Y. (1997) Molecular biology of the pore-forming cytolysins from *Staphylococcus aureus* α-hemolysin and γ-hemolysins and leukocidin, *Biosci. Biotechnol. Biochem. 61*, 565−572.
6. Sugawara, N., Tomita, T., and Kamio, Y. (1997) Assembly of *Staphylococcus aureus* γ-hemolysin into a pore-forming ring-shaped complex on the surface of human erythrocytes, *FEBS Lett. 410*, 333−337.
7. Olson, R., Nariya, H., Yokota, K., Kamio, Y., and Gouaux, E. (1999) Crystal structure of staphylococcal LukF delineates conformational changes accompanying formation of a transmembrane channel, *Nat. Struct. Biol. 6*, 134−140.
8. Nguyen, V. T., and Kamio, Y. (2004) Cooperative Assembly of β-Barrel Pore-Forming Toxins, *J. Biochem. (Tokyo) 136*, 563−567.
9. Sugawara-Tomita, N., Tomita, T., and Kamio, Y. (2002) Stochastic assembly of two-component staphylococcal γ-hemolysin into heteroheptameric transmembrane pores with alternate subunit arrangements in ratios of 3:4 and 4:3, *J. Bacteriol. 184*, 4747−4756.
10. Comai, M., Dalla Serra, M., Coraiola, M., Werner, S., Colin, D. A., Monteil, H., Prevost, G., and Menestrina, G. (2002) Protein engineering modulates the transport properties and ion selectivity of the pores formed by staphylococcal γ-hemolysin in lipid membranes, *Mol. Microbiol. 44*, 1251−1267.
11. Miles, G., Movileanu, L., and Bayley, H. (2002) Subunit composition of a bicomponent toxin: staphylococcal leukocidin forms an octameric transmembrane pore, *Protein Sci. 11*, 894−902.
12. Jayasinghe, L., and Bayley, H. (2005) The leukocidin pore: evidence for an octamer with four LukF subunits and four LukS subunits alternating around a central axis, *Protein Sci. 14*, 2550−2561.
13. Pedelacq, J. D., Maveyraud, L., Prevost, G., Baba-Moussa, L., Gonzalez, A., Courcelle, E., Shepard, W., Monteil, H., Samama, J. P., and Mourey, L. (1999) The structure of a *Staphylococcus aureus* leucocidin component (LukF-PV) reveals the fold of the water-soluble species of a family of transmembrane pore-forming toxins, *Struct. Folding Des. 7*, 277−287.
14. Song, L., Hobaugh, M. R., Shustak, C., Cheley, S., Bayley, H., and Gouaux, J. E. (1996) Structure of staphylococcal α-hemolysin, a heptameric transmembrane pore, *Science 274*, 1859−1866.
15. Nguyen, T. V., Kamio, Y., and Higuchi, H. (2003) Single-molecule imaging of cooperative assembly of staphylococcal γ-hemolysin on erythrocyte membranes, *EMBO J. 19*, 4968−4979.
16. Monma, N., Nguyen, V. T., Kaneko, J., Higuchi, H., and Kamio, Y. (2004) Essential Residues, W177 and R198, of LukF for Phosphatidylcholine-Binding and Pore-Formation by Staphylococcal γ-Hemolysin on Human Erythrocyte Membranes, *J. Biochem. (Tokyo) 136*, 427−431.
17. Nguyen, T. V., Higuchi, H., and Kamio, Y. (2002) Controlling pore assembly of staphylococcal γ-hemolysin by low temperature and by disulfide bond formation in double-cysteine LukF mutants, *Mol. Microbiol. 45*, 1485−1498.
18. Kaneko, J., Ozawa, T., Tomita, T., and Kamio, Y. (1997) Sequential binding of Staphylococcal γ-hemolysin to human erythrocytes and complex formation of the hemolysin on the cell surface, *Biosci. Biotechnol. Biochem. 61*, 846−851.
19. Nguyen, H. A., and Higuchi, H. (2005) Motility of myosin V regulated by the dissociation of single calmodulin, *Nat. Struct. Mol. Biol. 12*, 127−132.
20. Valeva, A., Weisser, A., Walker, B., Kehoe, M., Bayley, H., Bhakdi, S., and Palmer, M. (1996) Molecular architecture of a toxin pore: a 15 residue sequence lines the transmembrane channel of Staphylococcal alpha-toxin, *EMBO J. 15*, 1857−1864.
21. Valeva, A., Palmer, M., and Bhakdi, S. (1997) Staphylococcal alpha-toxin: formation of the heptameric pore is partially cooperative and proceeds through multiple intermediate stages, *Biochemistry 36*, 13298−13304.
22. Schindel, C., Zitzer, A., Schulte, B., Gerhards, A., Stanley, P., Hughes, C., Koronakis, V., Bhakdi, S., and Palmer, M. (2001) Interaction of *Escherichia coli* hemolysin with biological mem-

branes. A study using cysteine scanning mutagenesis, *Eur. J. Biochem. 268*, 800−808.
23. Gouaux, E. (1997) α-Hemolysin, γ-hemolysin, and leukocidin from *Staphylococcus aureus*: distant in sequence but similar in structure, *Protein Sci. 6*, 2631−2635.
24. van der Goot, F. G. (2001) *Pore-forming toxins*; Springer-Verlag, Berlin and Heidelberg, Germany.
25. Sellman, B. R., Kagan, B. L., and Tweten, R. K. (1997) Generation of a membrane-bound, oligomerized prepore complex is necessary for pore formation by *Clostridium septicum* alpha toxin, *Mol. Microbiol. 23*, 551−558.
26. Ramachandran, R., Tweten, R. K., and Johnson, A. E. (2004) Membrane-dependent conformational changes initiate cholesterol-dependent cytolysin oligomerization and intersubunit β-strand alignment, *Nat. Struct. Mol. Biol. 11*, 697−705.
27. Czajkowsky, D. M., Hotze, E. M., Shao, Z., and Tweten, R. K. (2004) Vertical collapse of a cytolysin prepore moves its transmembrane β-hairpins to the membrane, *EMBO J. 23*, 3206−3215.
28. Miller, C. J., Elliott, J. L., and Collier, R. J. (1999) Anthrax protective antigen: prepore-to-pore conversion, *Biochemistry 38*, 10432−10441.
29. Shepard, L. A., Shatursky, O., Johnson, A. E., and Tweten, R. K. (2000) The mechanism of pore assembly for a cholesterol-dependent cytolysin: formation of a large prepore complex precedes the insertion of the transmembrane beta-hairpins, *Biochemistry 39*, 10284−10293.
30. Hotze, E. M., Wilson-Kubalek, E. M., Rossjohn, J., Parker, M. W., Johnson, A. E., and Tweten, R. K. (2001) Arresting pore formation of a cholesterol-dependent cytolysin by disulfide trapping synchronizes the insertion of the transmembrane beta-sheet from a prepore intermediate, *J. Biol. Chem. 276*, 8261−8268.
31. Cabiaux, V., Buckley, J. T., Wattiez, R., Ruysschaert, J. M., Parker, M. W, and van der Goot, F. G. (1997) Conformational changes in aerolysin during the transition from the water-soluble protoxin to the membrane channel, *Biochemistry 36*, 15224−15232.
32. Palmer, M., Harris, R., Freytag, C., Kehoe, M., Tranum-Jensen, J., and Bhakdi, S. (1998) Assembly mechanism of the oligomeric streptolysin O pore: the early membrane lesion is lined by a free edge of the lipid membrane and is extended gradually during oligomerization, *EMBO J. 17*, 1598−1605.
33. Walker, B., Krishnasastry, M., Zorn, L., and Bayley, H. (1992) Assembly of the oligomeric membrane pore formed by staphylococcal α-hemolysin examined by truncation mutagenesis, *J. Biol. Chem. 267*, 21782−21786.
34. Montoya, M., and Gouaux, E. (2003) Beta-barrel membrane protein folding and structure viewed through the lens of α-hemolysin, *Biochim. Biophys. Acta 1609*, 19−27.

BI0514156